International Journal of Automotive Technology, Vol. 7, No. 2, pp. 167−172 (2006)

1229−9138/2006/026−07

VEHICLE DYNAMIC CONTROL ALGORITHM AND ITS IMPLEMENTATION ON CONTROL PROTOTYPING SYSTEM

Y. ZHANG*, C. YIN and J. ZHANG

The Institute of Automotive Engineering, Shanghai Jiaotong University, Shanghai 200240, China

(Received 20 June 2005; Revised 23 January 2006)

ABSTRACT−A design of controller for vehicle dynamic control (VDC) and its implementation on the real vehicle were introduced. The controller has been designed using a three-degrees-of-freedom (3DOF) yaw plane vehicle, and the control algorithm was implemented on the vehicle by control prototyping system dSPACE. A hybrid control algorithm, which makes full use of the advantages of robust and fuzzy control, was adopted in the control system. Field test results show that the performance of the vehicle handling dynamics with hybrid controller is improved obviously compared to that without VDC and with simple robust controller on skiddy roads (friction coefficients lower than 0.3).

KEY WORDS : Vehicle dynamic control, Control prototyping, Fuzzy-robust hybrid control

NOMENCLATURE

a	: distance from the centre of gravity (c.g.) to the front axle
b	: distance from the c.g. to the rear axle
a_y	: vehicle lateral acceleration, positive towards right
v_x	: vehicle longitudinal velocity, positive forward
v_y	: vehicle lateral velocity, positive towards right
I_z	: vehicle moment of inertia about yaw axis
C_{ar}	: rear tire cornering tire stiffness
C_{af}	: front tire cornering tire stiffness
F_{sF}	: front tire lateral force
F_{sR}	: rear tire lateral force
m	: mass of the vehicle
α_f, α_r	: front tire slip angle, rear tire slip angle
ω_f, ω_{rd}	: yaw rate, optional yaw rate
β, β_d	: vehicle sideslip angle, optional sideslip angle
δ_f	: front tire steering angle
M_z	: yaw moment generated by active brake

1. INTRODUCTION

VDC system is an active safety system for road vehicles. It stabilizes the lateral dynamic behavior of a vehicle in emergency situations and prevent it from spinning, drifting and rolling over (Bosch, 1999; Zanten Van, 1996; Chung *et al.*, 2004). The benefits from the use of VDC in improving vehicle stability in emergency situations have been well documented (Van Zantan, 2000; Aleksander and Mark, 2002; Motoki and Masao, 2001). In this paper, hybrid control algorithm for VDC and its implementation on real vehicle with Control Prototyping system dSPACE are introduced.

Critical lateral motion of a vehicle refers to the situation in which the tire-road adhesion can no longer be sustained. In such situations, the sideslip angle of body grows and the sensitivity of the yaw moment with respect to the steering angle suddenly diminishes. An addition of the steering angle can no longer increase the yaw moment that is necessary to restore the vehicle stability. However the active brake control can generate a yaw moment directly by developing longitudinal Force(s) on one side of vehicle, thus restoring the vehicle stability. This is the so-called Vehicle Dynamic Control system (Bosch, 1999; Aleksander and Mark, 2002), and many efforts are being made in automotive industries to develop it. The design of the control systems that drive active brake is a big challenge, given the fact that there are multiple actuators, sensors and control objectives, in addition to nonlinear vehicle dynamics and varying coefficient of friction between the tires and road. Because the dynamics of the vehicle close to being unstable is a complex nonlinear system, it is very difficult to control the nonlinear and uncertain system with the simple robust controller (Jang *et al.*, 2003). Hence, a hybrid robust fuzzy control is applied to VDC system. The control system includes a state feedback controller and a robust fuzzy controller (Chih *et al.*, 2003; Sylvia and Henryk, 2003). A state feedback gain is designed to guarantee the

**Corresponding author.* e-mail: blue_hawk@263.net

system stability and the desired control performance of the nominal system. In addition, a fuzzy law is used to tune a robust gain so as to cope with the system uncertainties and model errors. This fuzzy law is derived from human experts' knowledge. Compared with other robust controllers, the control method has the advantage of small chattering of control effort, system stability and performance robustness.

The controller drives twelve actuators which regulate the hydraulic pressure of the four wheels and the two relays which control the voltage supply of the motor and the valve, based on the speed of the four wheels, the forward acceleration, the lateral acceleration, the yaw rate, the steering wheel angle, and the brake pressure of the driver. The control objective is to minimize the sideslip angle and the modeling error of the yaw rate to obtain vehicle stability and path trace.

Finally, based on the field test result of the vehicle using the control algorithm prototyping, we demonstrate the feasibility and the good performance of the control algorithm implemented on the dSPACE system with DS1005 PowerPC 750 processor boards and DS2210 interface board (dSPACE).

2. VEHICLE MODEL FOR CONTROLLER DESIGN

The vehicle used for control system design is modeled as a 3-DOF planar bicycle model with linear tire model (Yi *et al.*, 2003). Figure 1 shows the planar vehicle model with three degree-of-freedom (3-DOF), i.e., the yaw, lateral, and longitudinal motions.

The governing equations of the lateral and yaw motions can be expressed as follows:

$$m(\dot{v}_y + v_x\omega_r) = 2F_{sF}\cos\delta_f + 2F_{sR}$$

$$I_z\dot{\omega}_r = 2aF_{sF}\cos\delta_f - 2bF_{sR}$$

and

$$mv_x(\dot{\beta} + \omega_r) = -2C_{af}\left(\beta + \frac{a\omega_r}{v} - \delta_f\right) - 2C_{ar}\left(\beta - \frac{b\omega_r}{v_x}\right)$$

$$I_z\dot{\omega}_r = -2aC_{af}\left(\beta + \frac{a\omega_r}{v_x} - \delta_f\right) + 2bC_{ar}\left(\beta - \frac{b\omega_r}{v_x}\right)$$

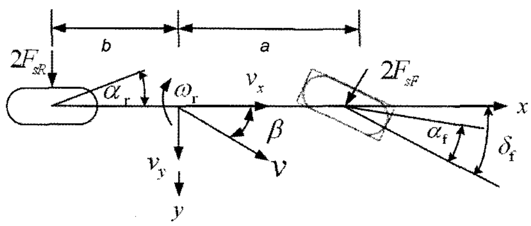

Figure 1. A three degree-of-freedom vehicle model in plane motion.

3. CONTROL SYSTEM DESIGN

3.1. Fundamental Control Structure

In order to improve the handling and stability of the vehicle, the sideslip angle and the modeling error of yaw rate are controlled to be minimal. The direct yaw moment generated by the longitudinal forces on one side of vehicle is employed as the control input to make actual responses approach the desired values. Figure 2 shows the block diagram of this control system.

3.2. Design of Estimator for Body Sideslip Angle

It is absolutely essential to get the state signals of the vehicle, the yaw rate and body sideslip angle for the state feedback controller (Masato *et al.*, 2001). Of the two states for the controller, the yaw rate can be directly measured by the yaw rate sensor, but the body sideslip angle is not measurable. There are two approaches to estimate the body sideslip angle, one is the direct integration method and the other is model-based estimation method (Ali and Huei, 2004). The former is vulnerable to the drift problem caused by the accumulation of the sensor noise, but it can yield nonlinear dynamics. The latter normally yields accurate estimation only in the linear region of the tire characteristics. The direct integration method with calibrating the drift error by the model-based estimation is adopted in this study. Figure 3

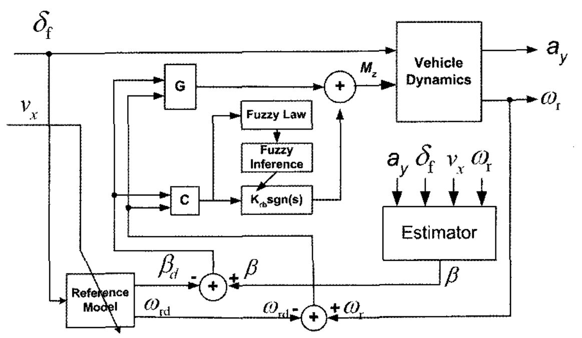

Figure 2. Block diagram of integrated control system.

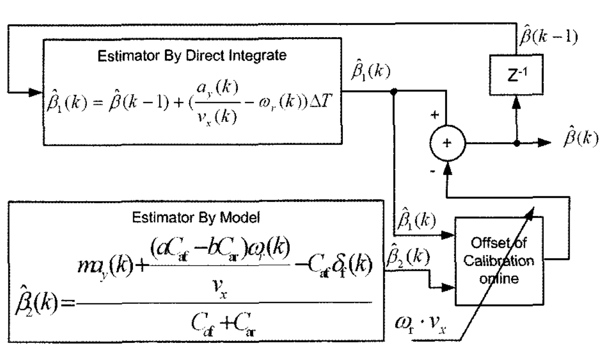

Figure 3. The block diagram of sideslip angle estimator.

is the block diagram of the body sideslip estimator.

3.3. The Controller System Design

Define $k_1=-2C_{af}$ $k_2=-2C_{ar}$

The control equations of the lateral and yaw motions with disturbances can be rewritten as follow:

$$\dot{\beta}=\frac{(k_1+k_2)}{mv_x}\beta+\left[\frac{(ak_1-bk_2)}{mv_x^2}-mv_x\right]\omega_r-\frac{k_1}{mv_x}\delta_f+d_1$$

$$\dot{\omega}_r=\frac{(ak_1-bk_2)}{I_z}\beta+\frac{(a^2k_1+b^2k_2)}{v_xI_z}\omega_r-\frac{ak_1}{I_z}\delta_f+\frac{M_z}{I_z}+d_2$$

In order to simplify the equations, Define the state, input, disturbances and matrix A B as

$$\boldsymbol{x}=\begin{pmatrix}\beta\\ \omega_r\end{pmatrix}\quad \boldsymbol{u}=\begin{pmatrix}\delta_f\\ M_z\end{pmatrix}\quad \boldsymbol{d}=\begin{pmatrix}d_1\\ d_2\end{pmatrix}$$

$$A=\begin{pmatrix}a_{11} & a_{12}\\ a_{21} & a_{22}\end{pmatrix}\quad \boldsymbol{B}=\begin{pmatrix}b_{11} & b_{12}\\ b_{21} & b_{22}\end{pmatrix}$$

$$a_{11}=\frac{(k_1+k_2)}{mv_x}\quad a_{12}=\frac{(ak_1+bk_2)}{mv_x^2}-mv_x$$

$$a_{21}=\frac{(ak_1-bk_2)}{I_z}\quad a_{22}=\frac{(a^2k_1+b^2k_2)}{v_xI_z}$$

$$b_{11}=-\frac{k_1}{mv_x}\quad b_{12}=0\quad b_{21}=-\frac{ak_1}{I_z}\quad b_{22}=\frac{I}{I_z}$$

The system model rewrite as

$$\dot{\boldsymbol{x}}=\boldsymbol{A}\boldsymbol{x}+\boldsymbol{B}\boldsymbol{u}+\boldsymbol{d}$$

Define the state error vector and the input as

$$\tilde{\boldsymbol{x}}=\boldsymbol{x}-\boldsymbol{x}_d\quad \boldsymbol{x}=\tilde{\boldsymbol{x}}+\boldsymbol{x}_d$$

where the optimal state and inputs as

$$\boldsymbol{x}_d=\begin{pmatrix}\beta_d\\ \omega_{rd}\end{pmatrix}\quad \boldsymbol{u}_d=\begin{pmatrix}\delta_f\\ 0\end{pmatrix}\quad \tilde{\boldsymbol{u}}=\begin{pmatrix}0\\ M_z\end{pmatrix}\quad \tilde{x}=\begin{pmatrix}\beta-\beta_d\\ \omega_r-\omega_{rd}\end{pmatrix}$$

The model is formulated as

$$\dot{\tilde{\boldsymbol{x}}}+\dot{\boldsymbol{x}}_d=\boldsymbol{A}\tilde{\boldsymbol{x}}+\boldsymbol{A}\boldsymbol{x}_d+\boldsymbol{B}\boldsymbol{u}_d+\boldsymbol{B}\tilde{\boldsymbol{u}}+\boldsymbol{d}$$

and $\dot{\boldsymbol{x}}_d=\boldsymbol{A}\boldsymbol{x}_d+\boldsymbol{B}\boldsymbol{u}_d$

Then the control model can be simplified as

$\dot{\tilde{\boldsymbol{x}}}=\boldsymbol{A}\tilde{\boldsymbol{x}}+\boldsymbol{B}\tilde{\boldsymbol{u}}+\boldsymbol{d}$ where $d\in R^n$

and $\tilde{\boldsymbol{u}}=\tilde{\boldsymbol{u}}_{fb}+\tilde{\boldsymbol{u}}_{rb}$

where the feedback controller $\tilde{\boldsymbol{u}}_{fb}$ is determined on the basis of the nominal model considering the disturbance-free case, while the robust controller $\tilde{\boldsymbol{u}}_{rb}$ compensates for the system uncertainty.

The linear feedback control law is designed as

$$\tilde{\boldsymbol{u}}_{fb}=\boldsymbol{G}\tilde{\boldsymbol{x}}$$

where $\boldsymbol{G}$ is the state feedback gain matrix which can be found from standard methods such as pole placement.

Then the closed-loop dynamic for the disturbance-free system is given by

$\dot{\tilde{\boldsymbol{x}}}=(\boldsymbol{A}+\boldsymbol{B}\boldsymbol{G})\tilde{\boldsymbol{x}}+\boldsymbol{d}$ where the closed-loop dynamics matrix $\boldsymbol{A}_c=(\boldsymbol{A}+\boldsymbol{B}\boldsymbol{G})$

has eigenvalues specialized in the left-half s-plane for the systems stability and desired responses.

Define denote the sliding surface as

$$S=C\begin{pmatrix}\dot{\tilde{x}}\\ \tilde{x}\\ 1\end{pmatrix}=\begin{pmatrix}(a_1\ 0) & (b_1\ 0) & c_1\\ (0\ a_2) & (0\ b_2) & c_2\end{pmatrix}\begin{pmatrix}\dot{\tilde{x}}\\ \tilde{x}\\ 1\end{pmatrix}=[s_1\ s_2]^T=0$$

The robust controller is designed as

$$\tilde{\boldsymbol{u}}_{rb}=-k_{rb}\operatorname{sgn}(s)=-(k_{rb1}\ k_{rb2})\begin{pmatrix}\operatorname{sgn}(s_1)\\ \operatorname{sgn}(s_2)\end{pmatrix}$$

where $k_{rb}\geq 0$ is estimated by the fuzzy control rules, which are based on result of previous research on the VDC, but for simple robust controller, k_{rb} is a constant.

Based on the result of previous researches on the VDC, The fuzzy control rules are in the following form:

Rule i: IF s is F_s^i, Then u is a_i

where F_s^i, i=1, 2, 3… m are the singleton control actions and is the label of the fuzzy set. The triangular-typed functions and singletons are used to define the membership functions of IF-part and THEN-part, which are depicted in Table1 and Figures 4(S1), (S2) and (krb), respectively.

The defuzzification of the control output is accomplished by the method of center-of-gravity

Table 1. the fuzzy control rules.

k_{rb1} / k_{rb2}		S_2					
		B0	B1	B2	B3	B4	B5
S_1	A0	C0 C0	C0 C1	C0 C2	C0 C4	C0 C4	C0 C5
	A1	C1 C0	C1 C1	C1 C2	C1 C4	C1 C4	C1 C5
	A2	C2 C0	C2 C0	C2 C1	C2 C3	C2 C3	C2 C4
	A3	C3 C0	C3 C0	C3 C1	C3 C1	C3 C2	C3 C2
	A4	C4 C0	C4 C0	C4 C1	C4 C1	C4 C1	C4 C1
	A5	C5 C0	C5 C0	C5 C0	C5 C1	C5 C1	C5 C2

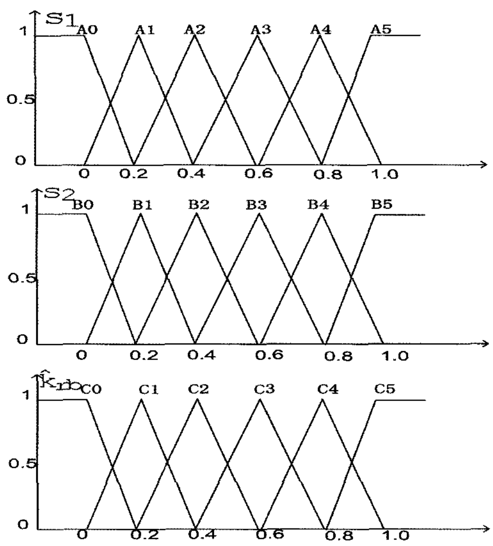

Figure 4. the membership functions of the inputs and output.

$$u_{fzj}(s)=\frac{\sum_{i=1}^{m} w_i a_i}{\sum_{i=1}^{m} w_i} \quad j=1,2$$

where w_i is the firing weight of the ith rule.

$$(k_{rb1}\ k_{rb2})=(k_{01}\times u_{fz1}\ \ k_{02}\times u_{fz2})$$

where k_{01} k_{02} is the gain for u_{fz1} u_{fz2}.

The M_{zi} generated by active braking usually is linear to F_{xi} and the wheel brake pressure P_i is linear to F_{xi} when the tire dynamics is linear. Hence, we can simply consider that P_i is linear to M_{zi}, and then

$M_z=\Sigma\lambda_i P_i$ where λ_i is coefficient which is affected by the friction coefficient and load distribution.

When the controller needs an additional yaw moment generated by active brake, the actuator gives an active brake pressure to the expected wheel. If the wheel tends to be locked during the increase of the brake pressure, the brake pressure will decrease according to the ABS control logic. The friction coefficient is estimated approximately according to the lateral acceleration when the vehicle tends to be unstable. The load distribution is also calculated approximately by lateral acceleration.

4. CONTROL PROTOTYPING USING DSPACE

The Control prototyping is performed with dSPACE control prototyping tool suite and Mathworks' Simulink. The MathWorks' Simulink is the core of the model-based design environment which allows the user to create a control algorithm in block-diagram form, and to perform non real-time simulation. The Real Time Workshop (RTW) is another module of the Matlab which can generate real-time C code for Simulink models. The real-time hardware and software of dSPACE are seamlessly integrated with Simulink/RTW, which provides a platform to run Simulink models in real-time with external input and output signals by Digital and Analog I/O of dSPACE. AutoBox is the special hardware environment for automotive control prototyping ,which is useful for control prototyping and vehicle dynamic real-time Hardware in Loop (HiL) simulation.

The control algorithm are very computationally intensive on the dSPACE DS1005 processor board with Motorola PowerPC 750 480 MHz processor. The analog signals are obtained from pressure sensors mounted in the wheel hydraulic cylinder and transferred to the Autobox via the A/D. The signal of steering angle is transferred to the Autobox via CAN bus. The signals of the wheel cylinder pressure, the steering angle, the lateral acceleration and the yaw rate are necessary for the analysis of the control prototyping test. The steering angle, the lateral acceleration and the yaw rate are necessary for control algorithm of the VDC runing on the processor. The controller gets the signals of the main cylinder pressure, the steering angle, the lateral acceleration and

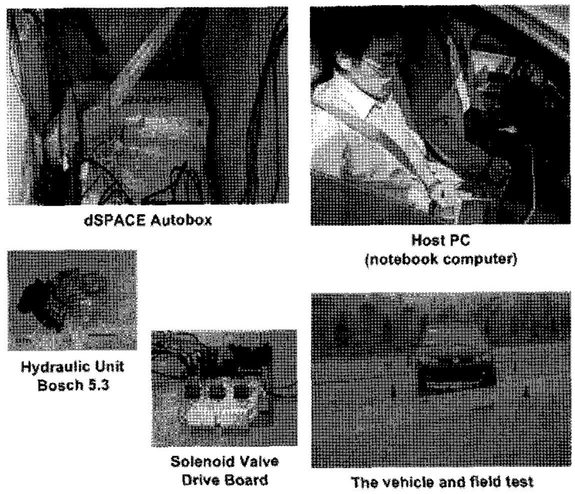

Figure 5. The pictures of field test.

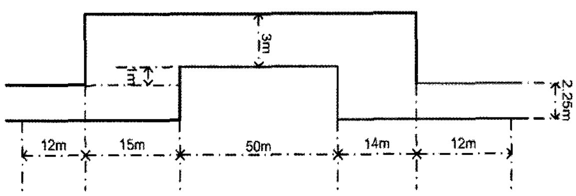

Figure 6. The desired path of double lane change test.

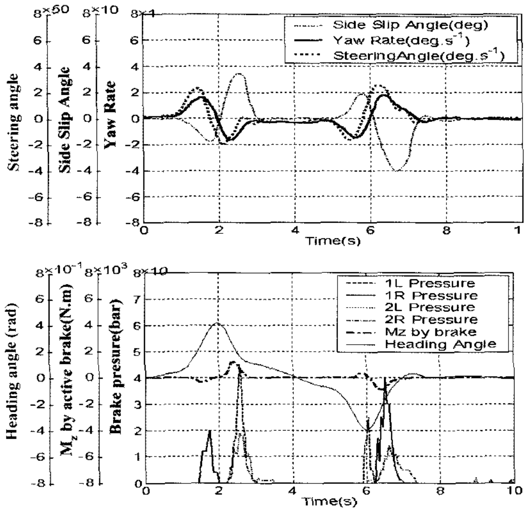

(a) The responds of vehicle with VDC of hybrid control

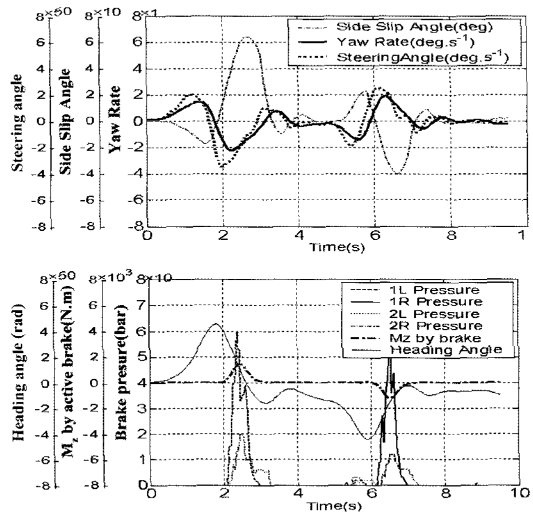

(b) The responds of vehicle with VDC of robust control

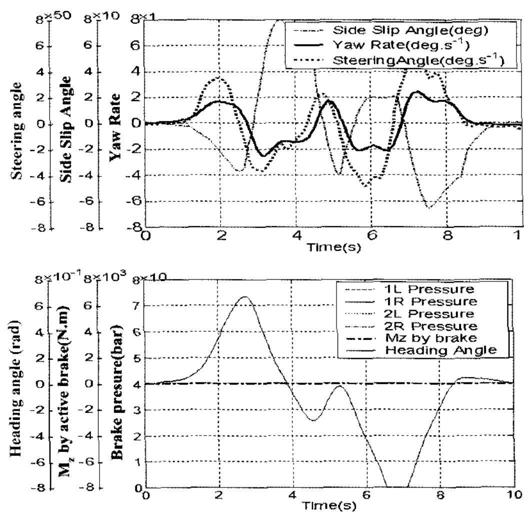

(c) The responds of vehicle without VDC

Figure 7. The double lane change at the speed of 50 km/h.

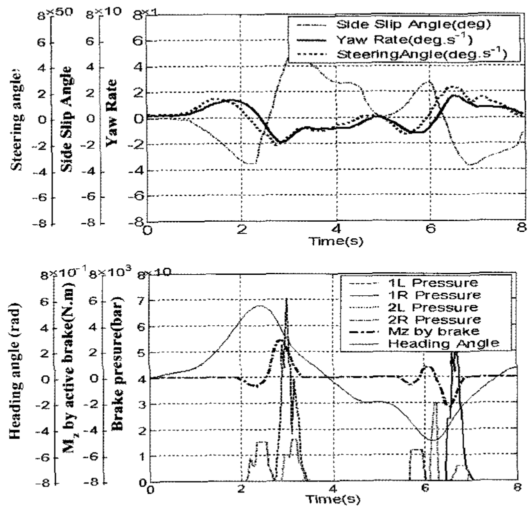

(a) The responds of vehicle with VDC of hybrid control

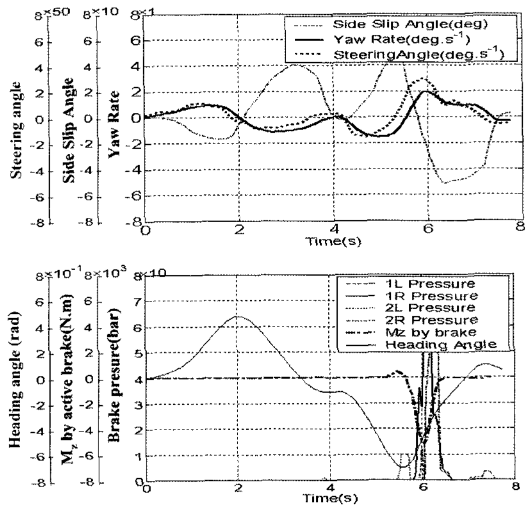

(b) The responds of vehicle with VDC of robust control

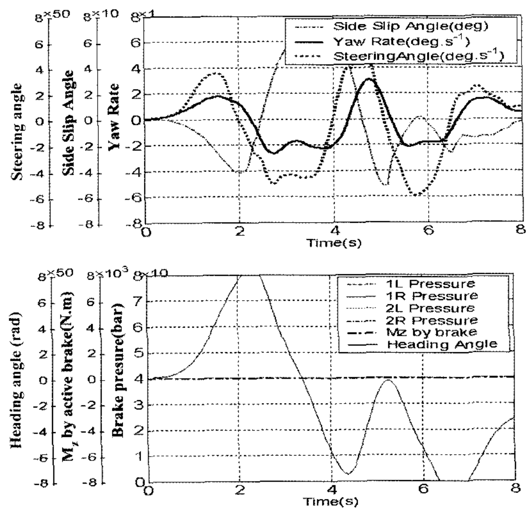

(c)The responds of vehicle without VDC

Figure 8. The double lane change at the speed of 70 km/h.

the yaw rate. The valve control logic is calculated by the control algorithm, and transferred to the drive board via Autobox digtal output. The drive board drives the hydraulic unit (Bosch ESP 5.3) to adjust the wheel brake pressure. Finally, the control prototyping system meets the target of the vehicle dynamics control. Figure(s) 5 is the field test pictures.

5. THE FIELD TEST RESULTS AND DISCUSSIONS

To demonstrate the feasibility and effectiveness of the control algorithm, the control algorithm is applied to vehicle field tests by dSPACE system. The testing vehicle is a small-size passenger car in the market, and the in-vehicle control system equipment are illustrated in Figure 5.

The double lane change test (Figure 6) was implemented on the road, which is formed by extending the ABS test road with leather flooring covered with water, and the friction coefficients is lower than 0.3. Figures 7, 8 are the results of the vehicle responses with and without VDC during the double lane change at the speed of 50 km/h and 70 km/h.

It shows that the vehicle without control responds with a larger side-slip angle and is absolutely out of control at the speed of 70 km/h. On the other hand, the side-slip and yaw rate controls stabilize the vehicle motion at the speed of 70 km/h, but the vehicle response with the hybrid controller is better than those with the robust controller and the vehicle with robust controller is inclined to unstable motion. The vehicle without VDC was not out of control at the speed of 50 km/h, but the sideslip angle of the vehicle with VDC is lower than that without VDC obviously and the vehicle response with the hybrid controller is better than that with the robust controller.

6. CONCLUSIONS

In this paper, a new control system design method for VDC has been introduced, and the control algorithm was implemented on dSPACE system. A differential braking strategy for the VDC controller has been designed using a 3DOF yaw plane vehicle model with wheel brake pressure inputs. In order to make the proposed controller robust to variable road conditions, a hybrid control method was adopted in the control system. The results of the experiment on skiddy roads at the speed of 50 km/h and 70 km/h have shown that the prototyping hybrid controller can produce superior performance than vehicles without VDC and those with simple robust controller in terms of brake actuation. The industrialization of the ECU with the proposed control system is the topics of ongoing research.

REFERENCES

Aleksander, H. and Mark, O. B. (2002). Improvements in vehicle through integrated control of chasis systems. *Int. J. Vehicle Design,* **29, 1/2**.

Ali, Y. U. and Huei, P. (2004). A study on lateral speed estimation methods. *Int. J. Vehicle Autonomous System,* **2, 1/2**.

Bosch (1999). *Vehicle Safety Systems for Passenger Cars.* ESP Electronic Stability Program Technical Instruction. Edn. Berlin. Germany.

Chung, T., Kim, J. and Yi, K. (2004). Human-in-the-loop evaluation of a vehicle stability controller using a vehicle simulator. *Int. J. Automotive Technology* **5, 2,** 109–114.

dSPACE webpage, www.dapace.com

Lin, C.-M. and Mon, Y.-J. (2003). Hybrid adaptive fuzzy controllers with application to robotic systems. *Fuzzy Sets and Systems,* **139,** 151–165.

Motoki, S. and Masao, N. (2001) Yaw-moment control of electric vehicle for improving handling and stability. *Japan Society Automotive Engineers Review,* **22,** 473–480.

Masato, A., Yoshio, K., Kazuasa, S., Yasuji, S., and Yoshimi, F. (2001). Side-slip control to stabilize vehicle lateral motion by direct yaw moment. *Japan Society Automotive Engineers Review,* **22,** 413–419.

Park, J.-H., Seo, S.-J. and Park, G.-T. (2003). Robust adaptive fuzzy controller for nonlinear system using estimation of bounds for approximation errors. *Fuzzy Sets and Systems,* **133,** 19–36.

Sylvia, K. R. and Henryk, F. (2003). Robust fuzzy logic control of mechanical systems. *Fuzzy Sets and Systems,* **133,** 77–108.

Van Zanten, A. T. (2000). *Bosch ESP Systems: 5 Years of Experience.* Society of Automotive Engineers, Inc. USA.

Van Zanten, A. T., Erhardt, R., Pfaff, G., Kost, F., Hartmann, U. and Ehret, T. (1996). Control aspects of the Bosch-VDC. *AVEC96*, 573–607.

Yi, K. S., Chung, T. Y., Kim, J. T. and Yi, S. J. (2003). An investigation into differential braking strategies for vehicle stability control. *Proc. Instn. Mech. Engrs. Part D: J. Automobile Engineering* **217, 12,** 1081–1094.